THREE UNIQUE FEL DESIGNS FOR THE NEXT GENERATION LIGHT SOURCE

G. Penn*, D. Arbelaez, J. Corlett, P.J. Emma, G. Marcus, S. Prestemon, M. Reinsch, R. Wilcox,
LBNL, Berkeley, CA 94720, USA
A. Zholents, ANL, Argonne, IL 60439, USA

Abstract

The NGLS is a next generation light source initiative spearheaded by the Lawrence Berkeley National Laboratory and based on an array of free-electron lasers (FEL) driven by a CW, 1-MHz bunch rate, superconducting linear accelerator. The facility is being designed to produce high peak and high average brightness coherent soft x-rays in the wavelength range of 1 nm – 12 nm, with shorter wavelengths accessible in harmonics or in expansion FELs. The facility performance requirements are based on a wide spectrum of scientific research objectives, requiring high flux, narrow-to-wide bandwidth, broad wavelength tunability, femtosecond pulse durations, and two-color pulses with variable relative timing and polarization, all of which cannot be encompassed in one FEL design. In addition, the cost of the facility requires building in a phased approach with perhaps three initial FELs and up to 9-10 FELs in the long term. We describe three very unique and complementary FEL designs here as candidates for the first NGLS configuration.

INTRODUCTION

The NGLS is conceived as a soft x-ray free-electron laser (FEL) user facility with high repetition rate and multiple beam lines. It will be based on a CW superconducting (SC) linac accelerating bunches with a 1-MHz bunch rate. These bunches will be distributed through an array of FEL beamlines. We present three distinct beamlines which each address different experimental needs.

The first beamline is self-seeded [1, 2]: it starts from noise like a SASE FEL, then has the radiation pass through a monochromator to seed a second stage. This scheme produces a large number of photons in a narrow bandwidth close to that specified by the monochromator. Not needing an external laser seed, this beamline is consistent with a high repetition rate, although heating of the monochromator optics may become an issue. The output pulse will have a duration roughly equivalent to the region of the beam where the electron energy is close to the nominal value and the peak current is high. This portion of the beam is referred to throughout this paper as the "usable" portion of the beam.

The second beamline uses a conventional external laser as a seed, which determines the output pulse timing and duration. The repetition rate is then limited to that of the external laser. X-rays are produced through two stages of high-gain harmonic generation (HGHG), with a "fresh-bunch" delay in between stages [3]. Due to the fresh bunch scheme, the output pulse duration cannot be more than about 1/3 of the usable portion of the beam. The duration can be as short as 5 fs. This provides control of both the pulse duration and bandwidth, which together remain close to the transform limit.

The third beamline also uses an external laser but in an unconventional manner, to generate energy and/or current modulations which then shape the output pulse during SASE [4]. The combination of the chirped electron beam and undulator tapering produces very narrow pulses, of a few femtoseconds, with a high bandwidth mostly due to a roughly linear frequency chirp. Because radiation tends to be suppressed outside of a small region of the beam, two independent pulses can be generated with independent control over their wavelengths and relative timing. The repetition rate is again limited by that of the external laser. This beamline can provide both pulses of a pump-probe measurement.

BEAMLINE PARAMETERS

The nominal parameters, which are broadly consistent with simulation studies, are shown in Table 1. However, the beamlines are designed to be able to handle a worse beam emittance, of up to 0.9 μm, or a lower peak current of 400 A. The energy spread is adjustable by the use of a laser heater [5] to damp out microbunching instabilities.

Table 1: Electron beam parameters, both slice and projected where relevant. The usable bunch duration is defined as the portion of the beam with relatively flat beam energy and high peak current.

	Whole Bunch	Slice
Bunch charge	300 pC	-
Electron energy	2.4 GeV	-
Energy spread	1.1 MeV	0.15 MeV
Transverse emittance	1.0 μm	0.6 μm
Peak current	-	500 A
Rms bunch length	50 μm	-
Usable bunch duration	300 fs	-

We focus on undulators using superconducting (SC) technology with relatively short undulator period, to provide a large tuning range with reasonably large dimensionless undulator parameter. Photon energy tuning will

* gepenn@lbl.gov

ISBN 978-3-95450-126-7

be accomplished by varying the undulator parameter K rather than by changing the electron energy. SC undulators have the advantage of being able to produce higher magnetic fields for a larger gap, especially for undulator periods shorter than 30 mm. SC undulators are also likely to be more robust when exposed to high average power approaching the MW level. The undulator sections are assumed to be 3.3 m long, with a break length between similar sections of 1.1 m for beam diagnostics and control.

The inner beam pipe diameter in the FEL beamline is assumed to be 4 mm, allowing for a magnetic gap of 6 mm. Going to larger beam pipe diameter would reduce the tuning range and probably require shifting to longer undulator periods. The shortest undulator period used in the beamlines described here is 20 mm, in which case we anticipate to be able to achieve an undulator parameter of $K = 5.0$ and a maximum magnetic field on axis of 2.7 T [6].

We consider an idealized, symmetric beam having a constant slice energy of 2.4 GeV and a current which ramps linearly to 500 A over an interval of 50 fs, is constant for 300 fs, and ramps back down linearly over 50 fs. In the figures, the constant current region is shown as the range from $t = 50$ fs to $t = 350$ fs. Resistive wall wakefields are modeled in the FEL beamline for a cold (4K) copper beampipe with a 4 mm inner diamter, but in this paper no consideration is taken of any effects in the linac which might lead to a less ideal distribution.

SELF-SEEDING SCHEME

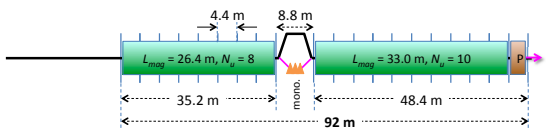

Figure 1: A schematic of the self-seeding configuration. The last undulator section is for polarization control.

The self-seeding scheme, shown in Fig. 1, breaks the undulators into two parts, with a monochromator and chicane in between. The noisy SASE bunching is eliminated by the chicane, and the monochromator selects a narrow bandwidth to seed the second stage. The monochromator should be roughly in the middle of the undulator length, constrained to be far enough downstream so that enough power gets through the monochromator to overcome shot noise, but not so far that the increased energy spread of the beam entering the second stage seriously degrades the FEL performance. To reach saturation, the total undulator length must be increased from that of a SASE beamline by enough to compensate for the following effects: the reduction in radiation energy due to both the narrower bandwidth and absorption by the optics; mismatch in the radiation transport; an effective loss in power by a factor of roughly 9 as some of the radiation couples to FEL modes which do not get amplified; and the slightly increased gain length in the second stage due to the increase in energy spread. For a monochromator with a resolution $R = 20,000$, which corresponds to a bandwidth of around 60 meV, and a 2% transport efficiency within this bandwidth, roughly 9 gain lengths must be added beyond what is needed to reach saturation in a straightforward SASE FEL. Only planar superconducting undulators are considered; polarization control can be obtained through the use of a cross-planar undulator at the very end of the beamline [7].

The beamline is designed to cover the range in photon energies from 200 eV up to 1.2 keV. At a resonant photon energy of 1.2 keV, the gain length is 2.0 m, and the effective FEL parameter is 4×10^{-4}. The effective shot noise power is 35 W. To ensure that shot noise is strongly suppressed in the second stage, we intend to keep the seeding power delivered by the monochromator above 3.5 kW.

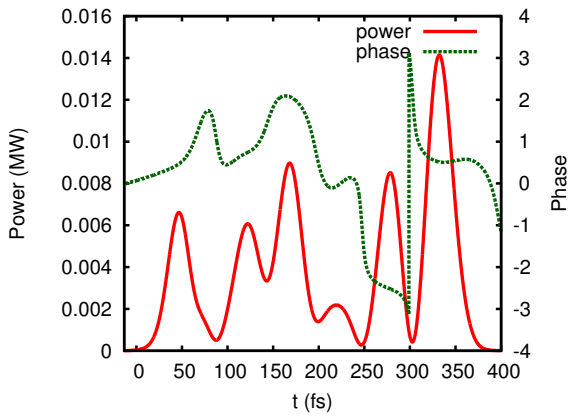

Figure 2: Temporal profile of power and phase immediately after the monochromator.

The radiation selected by the monochromator will act as the seed to be amplified in the second stage. At 1.2 keV, because the bunch duration is much longer than the coherence time of roughly 30 fs generated by the monochromator, the second stage is seeded by multiple spikes. The power and phase profiles coming out of the monochromator for a single simulation are shown in Fig. 2. The structure and total energy of this radiation will vary significantly from shot to shot, as it results from a filtering process on SASE radiation. In fact, because there are fewer longitudinal modes, the net energy fluctuation will be larger that of a SASE FEL. However, each mode is still contained within the monochromator bandwidth of roughly 60 meV.

This bandwidth is conserved during the second stage, although chirps in the electron bunch could alter the spectrum significantly. The power profile will vary shot to shot, but by a combination of reaching saturation and passing through multiple frequency spikes from the SASE stage, the power stability should be near the ten percent level even if the fine details of the spectrum vary significantly. In Fig. 3, the final power profile for the same simulation is compared to the power profile entering the monochromator. The spectra at various stages including the exit of the

ISBN 978-3-95450-126-7

monochromator are compared in Fig. 4. Unlike a SASE FEL, energy jitter could increase the power fluctuations because the photon energy is fixed by the monochromator. For the NGLS, the electrons are accelerated in a high repetition rate SC linac. It is expected that the energy jitter can be kept sufficiently low for this not to be a concern. Even for the self-seeded beamline, the energy only has to be accurate to well within the acceptance of the FEL, not that of the monochromator.

With the given choice for the location of the monochromator, the SASE radiation at that point is far from saturation and the energy spread generated in the first stage has little effect on the growth in the second stage. Even so, a MHz-rate beamline will impose over 2 W of average FEL power deposition on the monochromator optics which is an important factor to consider in the design of the optics.

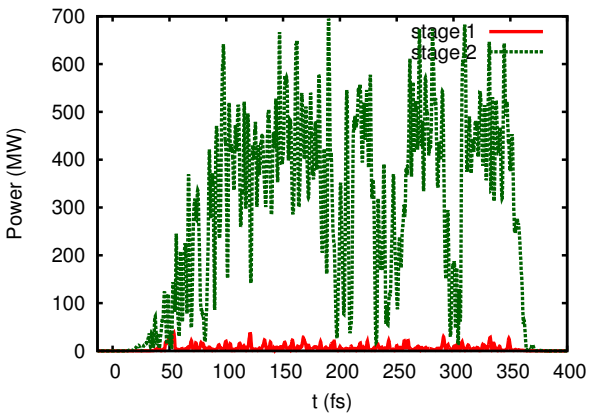

Figure 3: Power profiles just before the monochromator and at the end of the beamline.

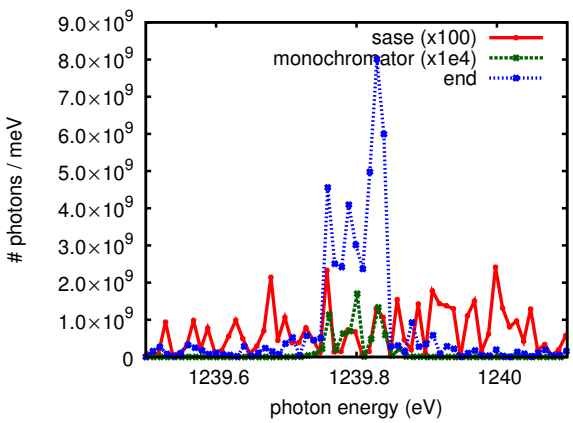

Figure 4: Comparison of spectrum at end of SASE stage, immediately after the monochromator, and at the end of the beamline.

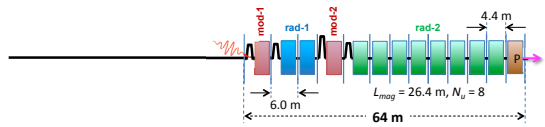

Figure 5: A schematic of the HGHG configuration.

HGHG SEEDED FEL

The HGHG scheme, shown in Fig. 5, uses two rounds of HGHG with a fresh bunch delay in between. This is similar to the recently operating FEL-2 beamline of FERMI@Elettra [8], but will push to even higher harmonics of the UV laser seed. The fresh bunch delay is critical because of the large energy spread which is induced at the end of the first HGHG stage. Ideally, the region of the bunch spoiled by the first HGHG stage will be well separated from the part of the bunch where the final x-ray pulse is radiated. To obtain the longest possible output pulse, these regions will have to overlap slightly.

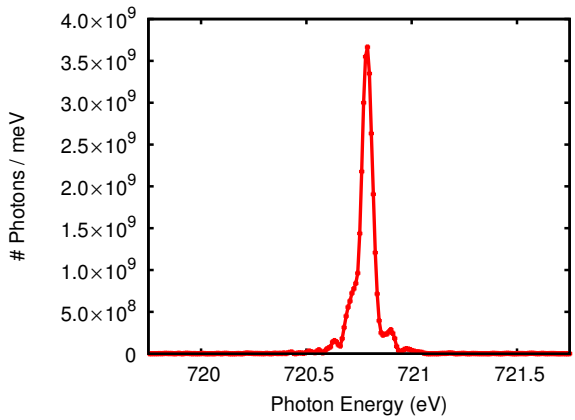

Figure 6: The spectral distribution of an HGHG x-ray pulse.

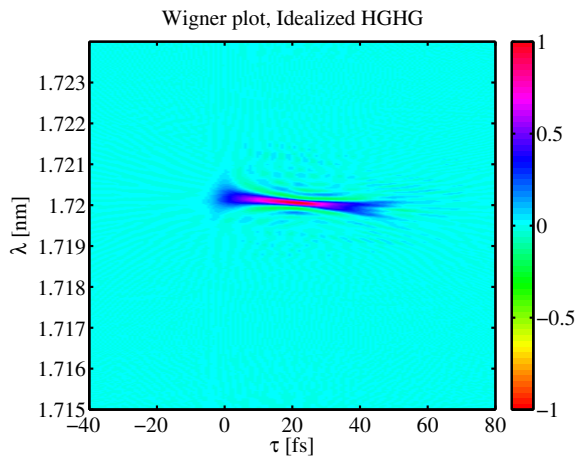

Figure 7: A Wigner plot of an HGHG x-ray pulse.

ISBN 978-3-95450-126-7

The first round of HGHG will normally be pushed to a higher jump in photon energy than the second round, because the end of the beamline where x-rays are produced is the most sensitive to energy spread. Going to a higher harmonic jump in the second stage will require more energy modulation in the second modulator, and this will lengthen the growth rate as well as reduce the saturated power. However, for a given beamline design, the maximum harmonic reach in the first stage will be limited by the energy spread. In particular, if both the energy spread at the start of the first radiator and the intermediate photon energy are too large, it will be difficult to produce enough power to properly modulate the beam after the fresh bunch delay. Results are shown for 720 eV photons, obtain by a jump of 18 in the first round of HGHG and 7 in the second round. The spectrum of the final x-ray pulse is shown in Fig. 6, and a Wigner plot of this pulse is shown in Fig. 7. The FWHM pulse length and bandwidth are 50 fs and 75 meV respectively; their product is twice the transform limit.

Various temporal profiles are shown in Fig. 8. The top figure shows various pulses at the different wavelengths, and also indicates the jump towards the head of the bunch after the fresh-bunch delay chicane. The input pulse has duration 100 fs, and the output pulse 50 fs. Also shown are the energy spread (middle figure) and bunching (bottom figure). Although the power profile of the earlier pulses appear to be well separated from those after the fresh-bunch delay, in terms of induced energy spread there is clearly some overlap. The spectrum of the pulse which passes through the fresh-bunch delay chicane is shown in Fig. 9. The spectral quality appears to be perfect, but upon subsequent harmonic multiplication the phase errors become significantly more apparent.

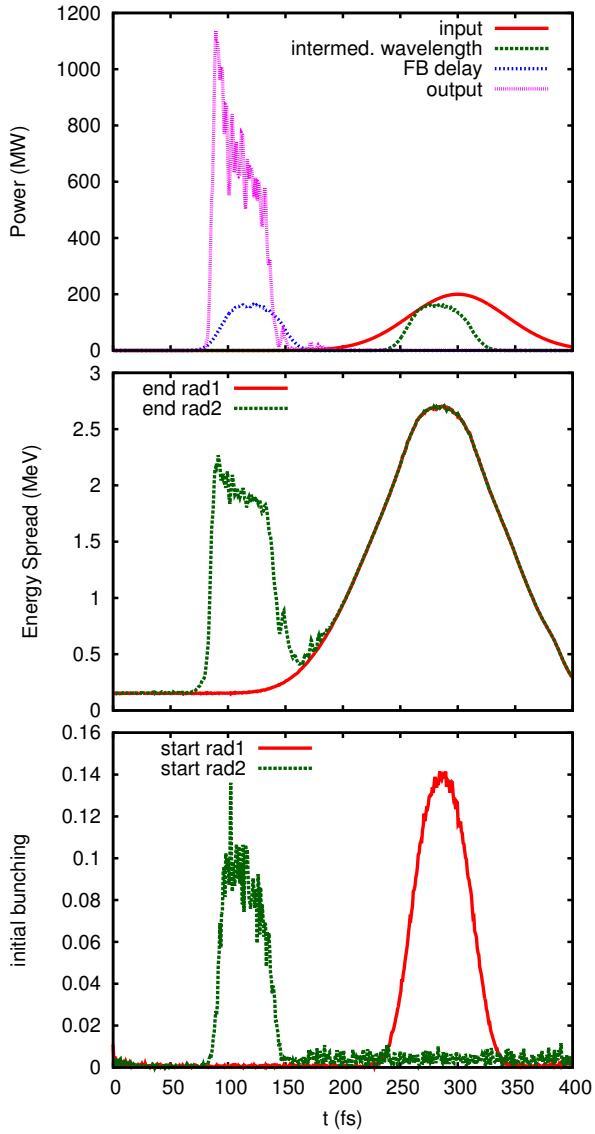

Figure 8: The radiation power profile (top) at various stages of the beamline. The input radiation is UV, the intermediate wavelength is 12 nm, and the output pulse has a photon energy of 720 eV. The induced energy spread (middle) is shown at the end of each radiator. The bunching (bottom) produced at the beginning of each radiator is also shown.

TWO-COLOR CHIRP-TAPER SCHEME

The two-color chirp-taper scheme, shown in Fig. 10, begins with a single-period undulator to modulate the beam. A few-cycle laser at 5 micron wavelength interacts strongly with a very short section of the electron bunch to generate a region with a strong energy chirp. The total energy swing in this few-femtosecond region is of order 10 MeV. Following an optional chicane to further manipulate the longitudinal distribution, the bunch enters a long x-ray amplifying section which has a strong taper, typically with increasing rather than decreasing undulator strength. If both the peak energy chirp and undulator taper are properly chosen, the taper serves two purposes: it suppresses SASE in the bulk of the electron bunch by ensuring that any radiation produced quickly falls outside of the FEL bandwidth, while supporting roughly a single SASE spike in the region with the appropriate chirp. The envelope of the original energy modulation must be short enough that nearby regions have either an energy chirp with either the wrong sign or otherwise significantly different from that of the target region, otherwise multiple spikes will be produced.

When the main pulse reaches saturation, it typically consists of a single spike well above the radiation power anywhere else in the beam. After the required undulator length to reach this point, another chicane is used to separate the electron bunch from the radiation pulse. The x-ray pulse can then be displaced away from the bunch trajectory, and a second 5-micron laser pulse is inserted to interact with the beam in another single-period undulator. A second amplifying section then produces another x-ray pulse. The largest source of degradation of bunch quality from the first stage is not SASE radiation, but rather energy spread growth from ISR. As long as the second laser pulse does not interact with the same electrons as the first, the second

ISBN 978-3-95450-126-7

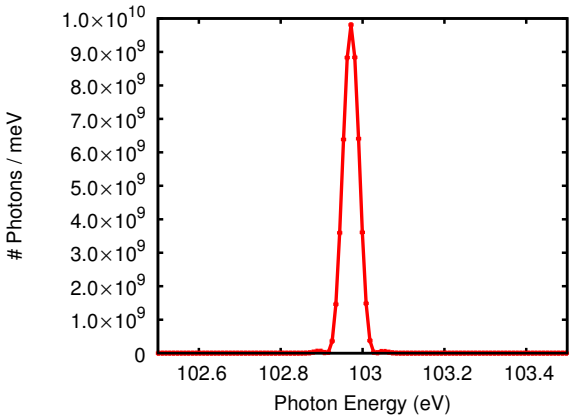

Figure 9: The spectral distribution of the pulse passing through the fresh-bunch delay.

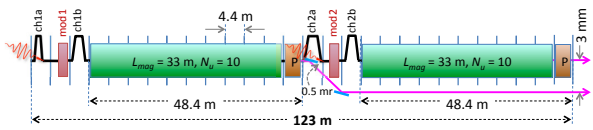

Figure 10: A schematic of the two-color chirp-taper configuration.

pulse-generating stage will proceed much as the first.

With only this small constraint on the timing of the second long-wavelength laser, there is a great deal of freedom in terms of the relative timing of the two x-ray pulses, and they could even be made synchronous in time. The photon energy of each pulse is determined by the tuning of the amplifying undulators, and is competely independent of the other pulse because two separate sets of undulators are used for amplification. Furthermore, because the two pulses are spatially separated, they can also be manipulated through x-ray optics to hit a sample at varying incident angles. This ability to perform multi-dimensional scans in time and wave vector at a high repetition rate opens up a broad range of scientific research. An example of a single x-ray pulse at 1 keV photon energy is shown in Figs. 11 and 12. In the first figure, the power profile is overlapped against the energy modulation of the beam. The second figure shows a Wigner plot of the pulse. The x-ray pulses are very short, typically several fs FWHM. They are not transform limited because of a large frequency chirp. The chirp is mostly linear and may itself be of some utility. If the chirp were used to compress the pulse shown in Fig. 12, the FWHM duration would be reduced from 2.5 fs to 0.6 fs, close to the transform limit.

CONCLUSIONS

We have described three different beamlines optimized for the NGLS, a next generation light source using a CW superconducting linac to deliver beam at a 1-MHz repetition rate to various FELs. Each FEL is compatible with identical electron bunch characteristics at 2.4 GeV, and offers distinct advantages and photon characteristics. Self-seeding has a tuning range of 0.2 – 1.2 keV, is compatible with the highest repetition rate, and offers over an order of magnitude more spectral brightness than SASE. It can also operate in pure SASE mode by removing the monochromator to increase the available photon energy up to 1.5 keV. The two-stage, HGHG cascade has a tuning range of 0.1 – 0.72 keV and produces pulses at close to the transform limit, although this becomes more challenging at the high end of the photon range. The timing and duration of the radiation is driven by an external UV laser and can be tightly controlled, but the repetition rate is limited to ∼100 kHz. The chirp-taper beamline suppresses radiation from the bulk of the beam to produce two short x-ray pulses with independent control over timing, photon energy and, with proper optics, angle of incidence. The pulses have a large frequency chirp, but otherwise have excellent mode quality. Because an external laser is used to manipulate the beam,

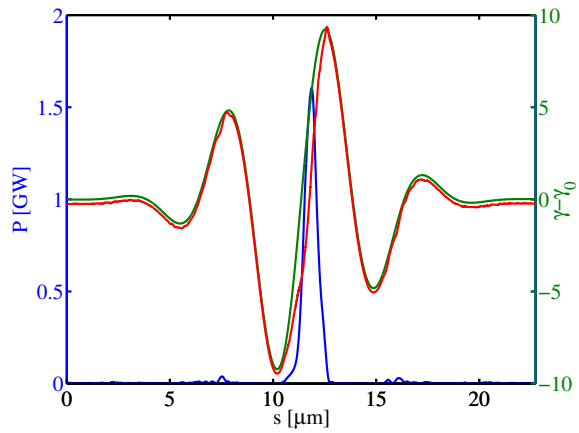

Figure 11: A sample power profile from the chirp-taper configuration, shown overlapping the energy profile both at the start and end of the x-ray amplifying stage.

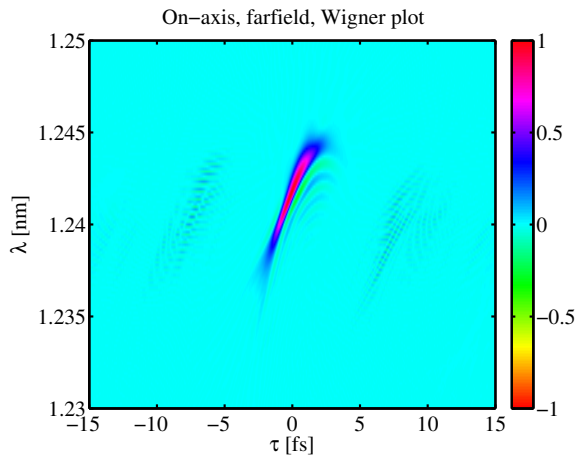

Figure 12: A Wigner plot of the x-ray pulse at 1 keV.

ISBN 978-3-95450-126-7

the repetition rate is again limited to ∼100 kHz. Each of these beamlines can produce of order 1 GW peak power.

ACKNOWLEDGMENTS

This work was supported by the Director, Office of Science, Office of Basic Energy Sciences, of the U.S. Department of Energy under Contract No. DE-AC02-05CH11231.

REFERENCES

[1] J. Feldhaus, E.L. Saldin, J.R. Schneider, E.A. Schneidmiller, and M.V. Yurkov, Optics Commun. **140** (1997) 341–352.

[2] J. Wu, P. Emma, Y. Feng, J. Hastings, and C. Pellegrini, "Staged self-seeding scheme for narrow bandwidth, ultra-short x-ray harmonic generation free electron laser at Linac Coherent Light Source," in *Proceedings of FEL2010, Malmö, Sweden*, Sweden, 2010, paper TUPB08, pp. 266–269.

[3] I. Ben-Zvi, K.M. Yang, and L.H. Yu, Nucl. Instrum. Methods A **318** (1992) 726–729.

[4] E.L. Saldin, E.A. Schneidmiller, and M.V. Yurkov, "Influence of an energy chirp on SASE FEL operation," in *Proceedings of FEL2005, Stanford, CA*, USA, 2005, paper TUPP006, pp. 258–261.

[5] Z. Huang, A. Brachmann, F.-J. Decker, Y. Ding, et al., Phys. Rev. ST Accel. Beams **13** (2010) 020703.

[6] S. Prestemon, D.R. Dietrich, S.A. Gourlay, P. Heimann, et al., "Design and evaluation of a short period Nb_3Sn superconducting undulator prototype," in *Proceedings of PAC2003, Portland, OR*, USA, 2003, paper MPPG010, pp. 1032–1034.

[7] K.-J. Kim, Nucl. Instrum. Methods A **445** (2000) 329–332.

[8] L. Giannessi, E. Allaria, L. Badano, D. Castranovo, et al., "First lasing of FERMI FEL-2 (1° stage) and FERMI FEL-1 recent results", in *Proceedings of FEL2012, Nara*, Japan, 2012, paper MOOB06, pp. 13–18.

ISBN 978-3-95450-126-7